

# Supplementary Material for Probabilistic Denoising-Enhanced and Parameterized Waveform Design for ISAC

Nghia Thinh Nguyen, Tri Nhu Do

## SUPPLEMENTARY MATERIAL

This document provides additional figures and technical details that support the manuscript “Probabilistic Denoising-Enhanced and Parameterized Waveform Design for ISAC”.

### I. ADDITIONAL FIGURES

Our system model consists of three objects: the radar, the user equipment (UE), and the terminal equipment (TE), as shown in Fig. 1. The radar is fixed while the TE and UE are moving.

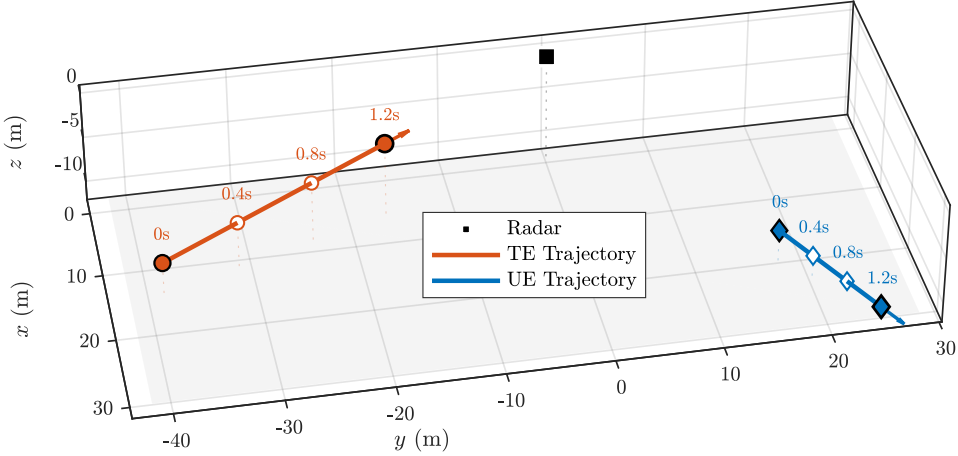


Fig. 1: The simulation map-based data of the PDISAC pipeline, including radar, TE, and UE.

The PDISAC waveform design is transmitted in the time domain, as can be seen in Fig. 2. The duration of each data symbol is transmitted sequentially by the PMCW waveform  $\vec{p}$  and the PMCW waveform integrated data symbol  $\vec{v}$ .

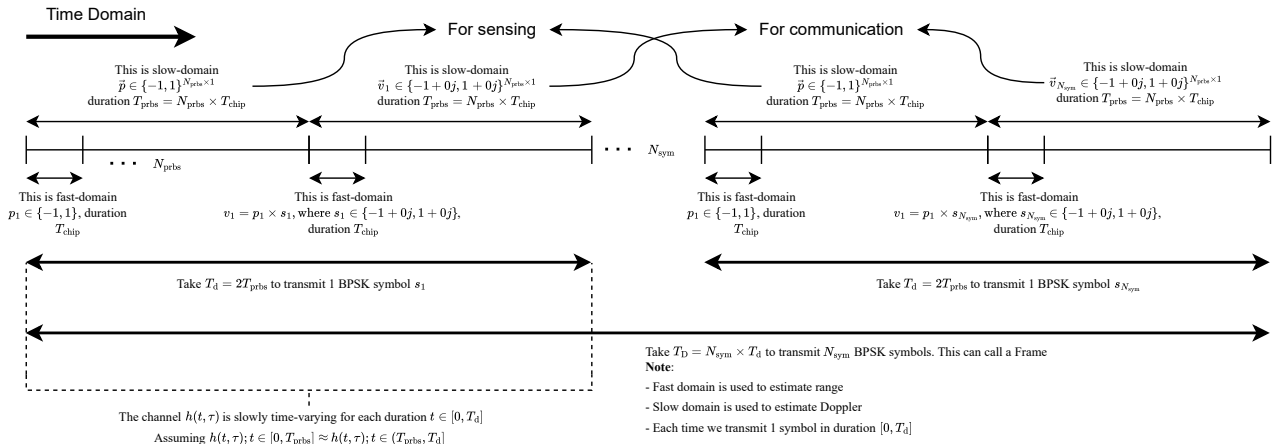


Fig. 2: Timeline of the ISAC waveform design.

Consider the range-Doppler estimation methods, i.e., the sequential estimator and CFAR. The accuracy of the estimated range and velocity depends on the resolution itself.  $\Delta r$  depends on the number of chips  $N_{\text{prbs}}$ , while  $\Delta\nu$  depends on the number of symbols  $N_{\text{sym}}$ . As presented in Fig. 4, the resolution of range and velocity decreases when  $N_{\text{prbs}}$  and  $N_{\text{sym}}$  increase. Besides, the symbol duration  $T_{\text{prbs}}$  also impacts the estimator methods.

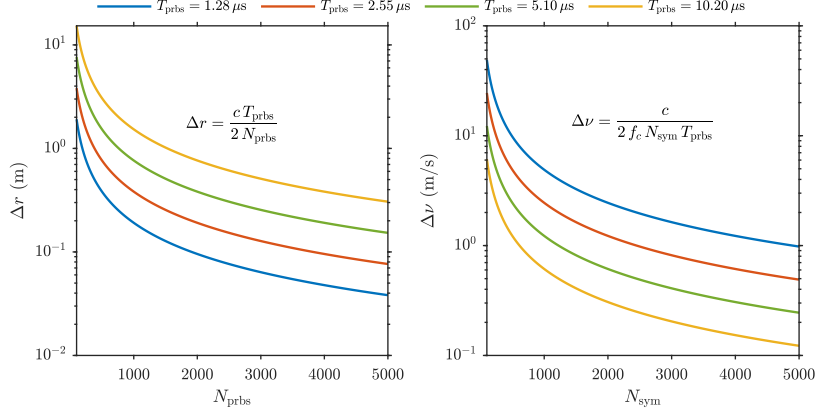


Fig. 3: The effect of  $N_{\text{prbs}}$  and  $N_{\text{sym}}$  on the resolution of the range  $\Delta r$  and velocity  $\Delta\nu$

According to Fig. 4, the sequential estimator method for range and velocity is presented from left to right. Given that the targets are TE and UE, the peak for ranges is shown in Fig. 4a. Then, based on each range peak, the velocity of each target is presented by Doppler peaks in Fig. 4b. According to Fig. 5, the CFAR method for range and velocity estimation is presented

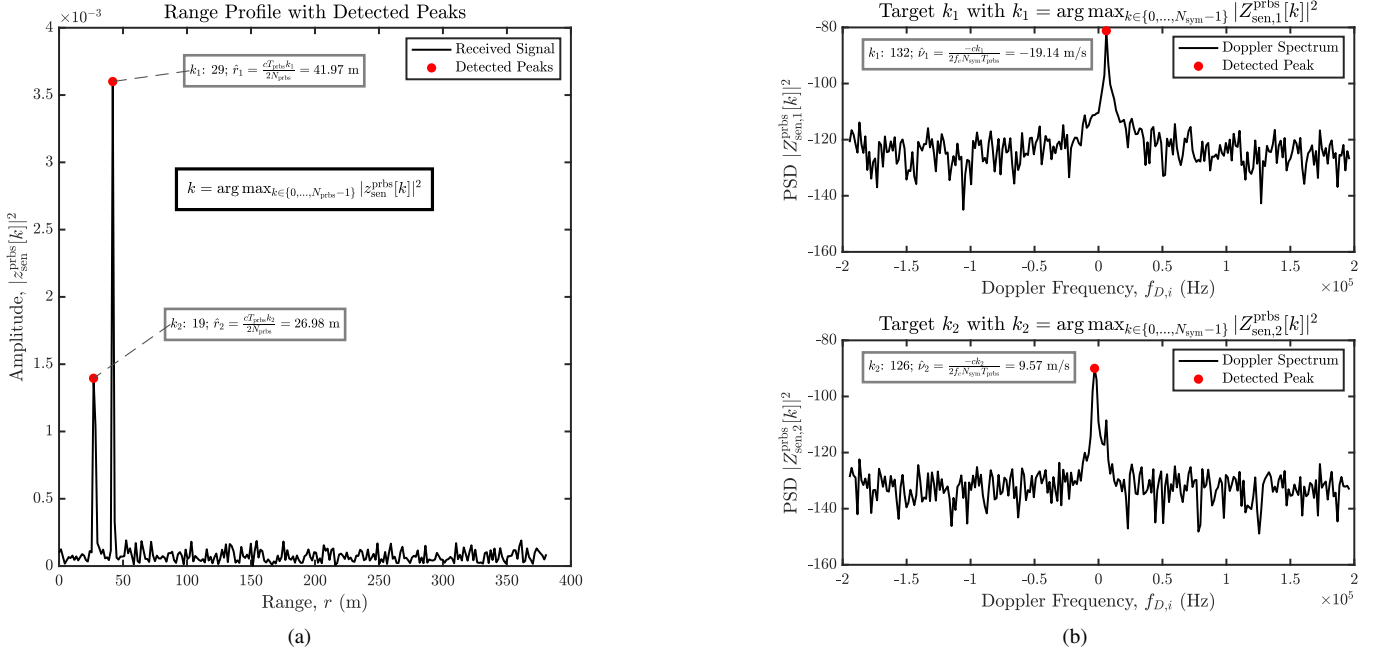


Fig. 4: (a) Range peak detection on Sequential Estimator (b) Doppler peak detection on Sequential Estimator

from left to right. The RD heatmap presents the potential targets, i.e., TE and UE, where the x-axis represents speed, and the y-axis represents distance, as shown in Fig. 5a. After applying CFAR, the targets are marked by blue circles, as shown in Fig. 5b.

In our proposal, the PDISAC pipeline is shown in Fig. 7. The first component is the sensing part of the ISAC framework, with the main purpose of estimating the range and velocity using CFAR. Given the observation in the TFR domain  $\mathbf{Y}_{\text{sen},\text{fast}}^{\text{prbs}}$ , we propose a denoising pipeline including preprocessing, training or inference, and postprocessing. In preprocessing, we produce the RD heatmap  $\mathbf{Y}_{\text{sen},\text{rd}}^{\text{prbs}}$  without applying the MF process as input to our proposed model, PDNet. The model architecture is split into training and inference architectures. The training architecture has an encoder block, extractor block, and decoder block, while the inference architecture has an extractor block and decoder block. The encoder block is removed during inference

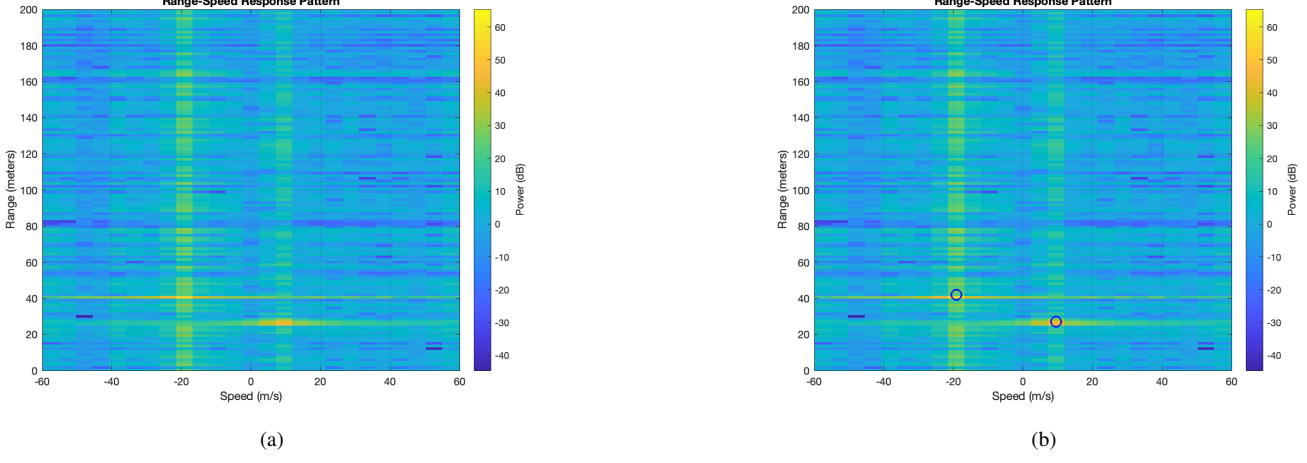


Fig. 5: (a) RD heatmap (b) Potential targets (TE, UE) on RD heatmap after CFAR process

to reduce computational cost and decrease latency in real time. The postprocessing step reproduces the MF output in the TFR domain,  $\hat{\mathbf{Z}}_{\text{sen},\text{fast}}^{\text{prbs}}$ , from the estimated RD heatmap  $\hat{\mathbf{Z}}_{\text{sen},\text{rd}}^{\text{prbs}}$ . The third block is the adversarial training process that improves the denoising model. From these three components, we provide three optimization formulations that are presented in the paper.

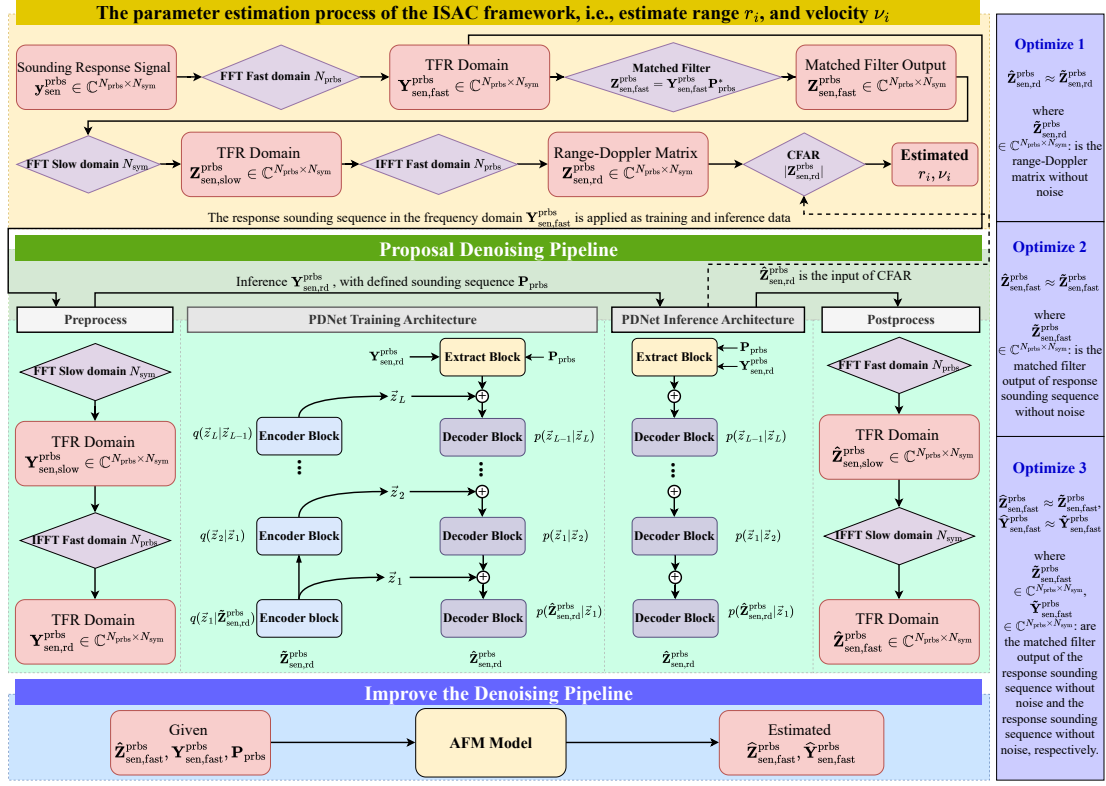


Fig. 6: The PDISAC denoising pipeline prototype comprises three main components: the conventional pipeline, the proposed denoising pipeline, and adversarial training to improve the proposed denoising pipeline, followed by three optimization problems.

To understand the characteristics of the observations and the engineered features in the paper, we visualize them in Fig. 7, showing pairs of real and imaginary images of the complex matrices. Meanwhile, Fig. 8 presents the Gaussian noise distribution before and after the MF process.

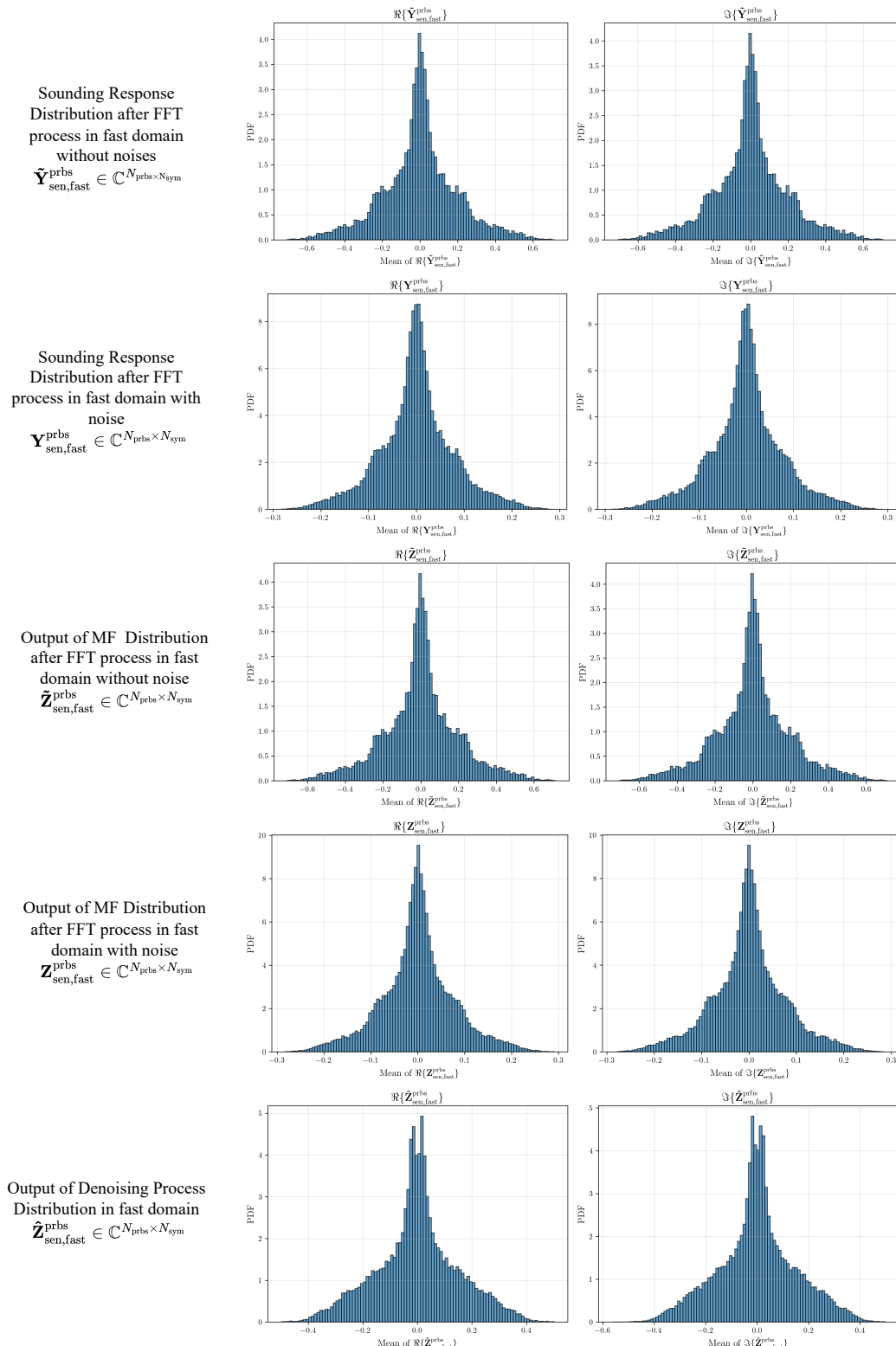


Fig. 7: Distribution of the observation and engineered features

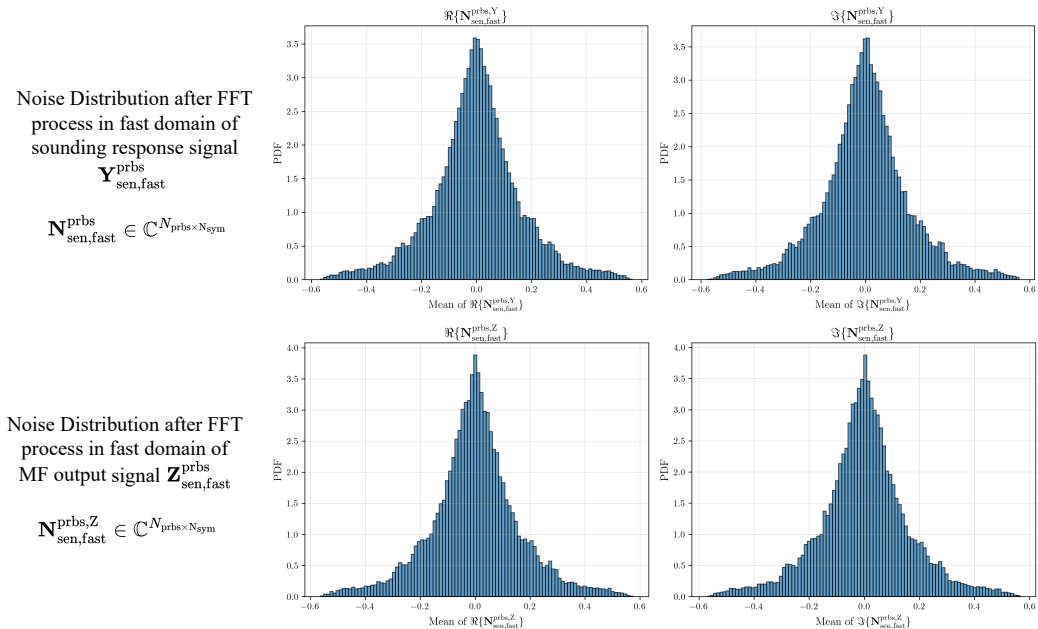


Fig. 8: Distribution of the noise factors